

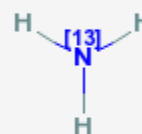
$[^{13}\text{N}]\text{Ammonia}$

$[^{13}\text{N}]\text{NH}_3$

Created: December 05, 2005

Updated: March 06, 2006

Chemical name: $[^{13}\text{N}]\text{Ammonia}$
Abbreviated name: $[^{13}\text{N}]\text{NH}_3$
Synonym:
Backbone: Compound
Target: Glutamine synthetase
Mechanism: Metabolic trapping in cells by enzymatic conversion to $[^{13}\text{N}]$ glutamic acid
Method of detection: PET
Source of signal: ^{13}N
Activation: No



Studies: ✓ *In vitro*
✓ Rodents
✓ Other non-primate mammals
✓ Non-human primates
✓ Humans

Click on the above structure for additional information in PubChem [<http://pubchem.ncbi.nlm.nih.gov>].

Background

[PubMed]

$[^{13}\text{N}]\text{Ammonia}$ ($[^{13}\text{N}]\text{NH}_3$) is a useful ^{13}N -labeled compound that has been developed as a positron emission tomography (PET) imaging agent for assessing regional blood flow in tissues (1-3). The compound is labeled with ^{13}N which is a positron emitter with a physical $t_{1/2}$ of 9.965 min. $[^{13}\text{N}]\text{NH}_3$ was approved by the United States Food and Drug Administration in 2000 for PET imaging of the myocardium under rest or pharmacologic stress conditions to evaluate myocardial perfusion in patients with suspected or existing coronary artery disease.

Ammonia is important in many metabolic activities of various organs and is involved in biochemical pathways leading to the production of amino acids, purines, and urea (4). Ammonia is produced in the body from the deamination of amino acids and the deamidation of amides (5). About 20% of urea produced in the body is converted to ammonia and carbon dioxide in the gut. Ammonia is absorbed and converted back to urea in the liver. It also plays a significant role in glutamine synthesis. Ammonia is produced from glutamine and other amino acids in the kidney. NH_3 , as a nonionic form, is freely permeable to all cell membranes (6). In an acidic environment, NH_3 accepts a proton and exists as NH_4^+ . With a dissociation constant ($\text{p}K_a$) of 9.3, NH_4^+ constitutes about 99% of the total ammonia ($\text{NH}_3 + \text{NH}_4^+$) concentration in the pH range of body fluids. As an ionized form, NH_4^+ is a relatively impermeable cation to cell membranes. The mechanism of cellular localization of $[^{13}\text{N}]\text{NH}_3$ is not entirely known. One known mechanism is cellular membrane diffusion of $[^{13}\text{N}]\text{NH}_3$ and then metabolic trapping of radioactivity with the conversion of ammonia to glutamine, glutamic acid and carbamyl phosphate (6-8).

Ammonia labeled with ^{13}N was first produced by Joliot and Curie (9, 10). The short $t_{1/2}$ of ^{13}N requires on-site cyclotron production of ^{13}N and a short synthesis time of $[^{13}\text{N}]\text{NH}_3$. After i.v. intravenous injection, $[^{13}\text{N}]\text{NH}_3$ rapidly clears from the circulation. It is taken up mainly by the myocardium, brain, liver, kidneys, and skeletal muscle (2, 6, 11, 12). In the myocardium and brain, $[^{13}\text{N}]\text{NH}_3$ is removed from the blood and metabolically trapped within the tissues. The apparent linear relationship between distribution of $[^{13}\text{N}]\text{NH}_3$ and the regional blood perfusion makes feasible the use of this radiotracer for imaging and measuring cerebral and myocardial blood flows.

Synthesis

[PubMed]

As early as 1934, Joliot and Curie (10) first produced $[^{13}\text{N}]\text{NH}_3$ by alpha particle irradiation and heating of boron nitride in sodium hydroxide. Later, $[^{13}\text{N}]\text{NH}_3$ was produced by deuteron irradiation of methane gas or metal carbides, which gave relatively low yields (4). A more efficient method is the proton irradiation of a natural water target $[^{16}\text{O}(\text{p},\alpha)^{13}\text{N}]$ (1, 13). In this procedure, $[^{13}\text{N}]\text{NH}_3$ is initially produced by hydrogen abstraction from the target water matrix. There is increasing production of oxo anions of nitrogen ($^{13}\text{NO}_3^-$ and $^{13}\text{NO}_2^-$) from radiolytic oxidation with increasing target dose. These oxo anions can be converted to $[^{13}\text{N}]\text{NH}_3$ in aqueous solution by use of reducing reagents such as DeVarda's alloy in sodium hydroxide or titanium(III) chloride/hydroxide. Ido et al. (14) first described a fully automated synthesis method with titanium(III) chloride used as the reducing agent. The radiochemical purity was >99.9% and the radiochemical yield was 87-91% within 10 min from the end of bombardment (EOB). $[^{13}\text{N}]\text{NH}_3$ also can be produced directly in the target water (in-target production) by adding free radical scavengers (ethanol, acetic acid, or hydrogen) to prevent the formation of the oxo anions. Wieland et al. (15) applied this method for $[^{13}\text{N}]\text{NH}_3$ production with the use of pressurized, dilute aqueous solutions of acetic acid and ethanol. Berridge et al.

(16) reported that the combination of hydrogen and ethanol was more effective than either alone at high beam doses. One limiting factor of the $[^{16}\text{O}(\text{p},\alpha)^{13}\text{N}]$ nuclear reaction is that the relatively small cross-section of the reaction requires accelerators/ cyclotrons of energies >10 MeV for production.

Ferrieri et al. (17) introduced a novel solid ^{13}C -enriched target for on-line $[^{13}\text{N}]\text{NH}_3$ production with use of the $^{13}\text{C}(\text{p},\text{n})^{13}\text{N}$ reaction. This nuclear reaction has a higher cross-section which can be used in accelerators/cyclotrons with <10 MeV energies. In their method, $[^{13}\text{N}]$ nitrogen gas was converted to $[^{13}\text{N}]\text{NH}_3$ by use of microwave radiation to dissociate the nitrogen gas in a hydrogen plasma. The reaction time was about 10 min, and radiochemical yield was 25% at 10 min after the EOB. Bida et al. (18) also used the method of $^{13}\text{C}(\text{p},\text{n})^{13}\text{N}$ reaction by placing enriched ^{13}C carbon powder between two frits and irradiating with a 10 MeV proton beam while water was pumped through the bed to extract the ammonia. Welch et al. (19) successfully produced $[^{13}\text{N}]\text{NH}_3$ with the use of $^{12}\text{C}(\text{d},\text{n})^{13}\text{N}$ reaction and a 7 MeV deuteron beam in aluminum carbide. Shefer et al. (20) and Dence et al (21). showed that a windowless, solid target could be irradiated with relatively low-energy (0.8-3.2 MeV) deuterons to produce $[^{13}\text{N}]\text{NH}_3$ by the $^{12}\text{C}(\text{d},\text{n})^{13}\text{N}$ reaction. This was accomplished by heating a graphite target in a stream of pure oxygen at 800°C , and $^{13}\text{NO}_2^-$ (99% radioactivity produced) was eluted with water and converted to $[^{13}\text{N}]\text{NH}_3$ with Raney nickel. The total extraction, trapping, and synthesis time was <17 min with a radiochemical purity of nearly 100%.

Mulholland et al. (22) reported a method of direct simultaneous production of $[^{13}\text{N}]\text{NH}_3$ and $[^{15}\text{O}]\text{H}_2\text{O}$ with the use of 26 MeV proton irradiation and a double liquid chamber. Suzuki et al. (23) designed an automated system that used 10 mM ethanol solution saturated with pure O_2 gas as the target and bombarded with 18 MeV protons. Krasikova et al. (24) reported an alternative method that used low-pressure methane gas (150-550 kPa) in the natural water target irradiated with protons. The radiochemical purity of $[^{13}\text{N}]\text{NH}_3$ was $>99\%$ even at very high beam currents. Firouzbakht et al. (25) used a cryogenic target containing frozen water for the $^{16}\text{O}(\text{p},\alpha)^{13}\text{N}$ reaction, and they found that this procedure (with beam currents from 1 μA to 20 μA) could produce $[^{13}\text{N}]\text{NH}_3$ directly because low temperature decreased radiolysis. The radiochemical purity of the $[^{13}\text{N}]\text{NH}_3$ produced was $>95\%$. When frozen carbon dioxide was irradiated, $>95\%$ of ^{13}N activity was in the form of nitrate and nitrite.

In Vitro Studies: Testing in Cells and Tissues

[PubMed]

Isolated arterially perfused rabbit interventricular septa ($n = 9$ at 28°C , $n = 10$ at 37°C) were used to study the relationship between blood flow, myocardial uptake, and the metabolism and clearance of $[^{13}\text{N}]\text{NH}_3$ (8). Analysis of the time-activity curves revealed that the $[^{13}\text{N}]\text{NH}_3$ kinetics were best described by three components. Component 1, with a short clearance $t_{1/2}$ of <7 min, was consistent with a freely diffusible NH_3 compartment. A large metabolic compartment was primarily responsible for component 3, which had a long clearance $t_{1/2}$ of 30 to 500 min. At 37°C and 15 min after injection, all radioactivity was essentially in component 3. In another study, glutamine syn-

thetase appeared to be responsible for retention of $[^{13}\text{N}]\text{NH}_3$ radioactivity in rabbit myocardium (26). In their study of $[^{13}\text{N}]\text{NH}_3$ uptake in myocardial single cells, Rauch et al. (27) found that in addition to metabolic trapping, the extraction of $[^{13}\text{N}]\text{NH}_3$ might also be influenced by cell membrane integrity, intracellular-extracellular pH gradient, and possibly an anion exchange system for bicarbonate.

Animal Studies

Rodents

[PubMed]

Imaging studies with $[^{13}\text{N}]\text{NH}_3$ in mice showed activity localization in the liver, myocardium, and bladder (12). The radioactivity cleared from the blood very rapidly with 85% clearance in the first minute, and 4.7% of the injected dose (ID) was excreted by the kidneys in 35 min. The biodistribution of $[^{13}\text{N}]\text{NH}_3$ was studied in rats (28). The rats were euthanized at different time intervals between 0.2 and 50 min after i.v. injection of 18.5 MBq (0.5 mCi)/kg of $[^{13}\text{N}]\text{NH}_3$ with an estimated specific activity of 74×10^5 to 148×10^5 GBq/mol (2×10^5 to 4×10^5 Ci/mol) at the EOB. The highest initial whole-organ radioactivities at 0.2 min after injection were in the lungs ($20.1 \pm 2.9\%$ ID $n=5$), kidneys ($13.6 \pm 1.2\%$ ID), and heart ($2.6 \pm 0.18\%$ ID), and at 50 min these values decreased to $1.51 \pm 0.17\%$ ID, $1.82 \pm 0.22\%$ ID, and $0.92 \pm 0.06\%$ ID, respectively. The radioactivity in the liver was $4.83 \pm 0.73\%$ ID at 0.2 min and then increased to a maximum of $14.4 \pm 0.7\%$ ID at 20 min. The radioactivity in the brain was $0.55 \pm 0.04\%$ ID at 0.2 min and then increased to a maximum of $0.89 \pm 0.1\%$ ID at 10 min.

Cooper et al. (29) studied the cerebral uptake and metabolism of $[^{13}\text{N}]\text{NH}_3$ in conscious rats, and they found that $[^{13}\text{N}]\text{NH}_3$ entered the brain from the blood largely by diffusion. This and other studies (30) indicated that the major route for metabolism of $[^{13}\text{N}]\text{NH}_3$ in the brain was incorporation into [amide- ^{13}N]glutamine. Lockwood et al. (31) showed that the brain-blood pH gradient had a major influence on the uptake of $[^{13}\text{N}]\text{NH}_3$ by the brain.

Other Non-Primate Mammals

[PubMed]

The localization of $[^{13}\text{N}]\text{NH}_3$ was studied in normal dogs by three methods of administration (inhalation, i.v., and s.c.) (4). All three methods showed similar imaging results. The radioactivity localization was mainly in the brain, heart, liver, and bladder. Approximately 10-20% of the ID was cleared rapidly from the blood by the kidneys and collected in the urinary bladder. The clearance $t_{1/2}$ of the kidneys was 7.7 to 10.6 min. In a dog study, Carter et al. (32) showed that increased blood pH increased brain uptake of $[^{13}\text{N}]\text{NH}_3$ and decreased blood pH decreased liver uptake of $[^{13}\text{N}]\text{NH}_3$. Rosenspire et al. (33) studied the metabolic fate of $[^{13}\text{N}]\text{NH}_3$ in dogs, and they found that urea was the predominant metabolite. Neutral amino acids (i.e., glutamine and asparagine) were the second most predominant metabolites. Schelbert et al. (34, 35) found a relatively linear relationship

between myocardial blood flow (from 0 to 500 ml/min/100 g in dogs) and myocardial $[^{13}\text{N}]\text{NH}_3$ radioactivity concentration. In comparison, the human physiologic range was from 0 to 350 ml/min/100 g. Other studies in dogs (36, 37) indicated that $[^{13}\text{N}]\text{NH}_3$ provided qualitative and quantitative information of myocardial blood flow comparable to data measured by microspheres and $[^{15}\text{O}]\text{H}_2\text{O}$.

The uptake kinetics of $[^{13}\text{N}]\text{NH}_3$ in the liver were studied in a pig model (38). A simplified circulatory model was proposed to estimate the hepatic clearance of $[^{13}\text{N}]\text{NH}_3$. The hepatic clearance was estimated to be 10.25 ± 1.84 ml/min/kg ($n = 4$).

Non-Human Primates

[PubMed]

The movement of $[^{13}\text{N}]\text{NH}_3$ from blood to brain was studied in rhesus monkeys (39). A regional residue detection model was proposed for the cerebral blood flow. The data revealed a diffusion limitation for the transport of $[^{13}\text{N}]\text{NH}_3$ from blood to brain because of the low permeability of $[^{13}\text{N}]\text{NH}_4^+$. Therefore at high flow rates the brain uptake of $[^{13}\text{N}]\text{NH}_3$ was no longer linear with flow increases.

Human Studies

[PubMed]

Harper et al. (12) performed imaging with 370 MBq (10 mCi) at the time of administration, (TOA) of $[^{13}\text{N}]\text{NH}_3$ in 2 healthy volunteers and showed that radioactivity localized in the myocardium, mediastinum, and liver. There was an initial moderate uptake in the lungs, and it was washed out after 5-10 min. In a metabolic study (33), 9 healthy male volunteers received iv. administration of 740 MBq (20 mCi at the TOA) of $[^{13}\text{N}]\text{NH}_3$ in normal saline. About $93.1 \pm 4.9\%$ ($n = 6$) of the blood radioactivity remained as $[^{13}\text{N}]\text{NH}_3$ within the first 2 min but was decreased to $50.2 \pm 18.9\%$ ($n = 5$) at 5 min after injection. At 1 min, the blood radioactivities associated with $[^{13}\text{N}]\text{glutamine}$ and $[^{13}\text{N}]\text{urea}$ were $3.0 \pm 2.4\%$ ($n = 6$) and $3.1 \pm 4.6\%$, respectively. By 5 min, the radioactivities for $[^{13}\text{N}]\text{glutamine}$ and $[^{13}\text{N}]\text{urea}$ had increased to $16.2 \pm 11.2\%$ ($n = 5$) and $32.7 \pm 10.0\%$, respectively. Lockwood et al. (11) reported a study of $[^{13}\text{N}]\text{NH}_3$ metabolism in 5 normal subjects with a dose of 370 MBq (10 mCi at the TOA) that showed that the rates of both radioactivity clearance from the vascular compartment and brain ammonia utilization were linear functions of its arterial concentration. About $47 \pm 3\%$ of $[^{13}\text{N}]\text{NH}_3$ radioactivity was taken up by the brain during a single pass from the arterial blood, and $7.4 \pm 0.3\%$ of $[^{13}\text{N}]\text{NH}_3$ was metabolized by the brain. Approximately 50% of the arterial $[^{13}\text{N}]\text{NH}_3$ was metabolized by the skeletal muscle. Changes in $[^{13}\text{N}]\text{NH}_3$ kinetics were reported in patients with tumors, hypopituitarism, and liver diseases [PubMed].

In 1980, Lockwood (40) reported the radiation absorbed doses of i.v. injection of $[^{13}\text{N}]\text{NH}_3$ with the use of body distribution data and the MIRD model. The urinary bladder wall was the critical organ with the highest total absorbed dose (0.014 mGy/MBq or 51 mrad/mCi). The whole body, liver, red

marrow, ovaries, and testes received 0.0015 mGy/MBq (5.5 mrad/mCi), 0.0046 mGy/MBq (17 mrad/mCi), 0.0015 mGy/MBq (5.4 mrad/mCi), 0.0027 mGy/MBq (9.8 mrad/mCi), and 0.00027 mGy/Bq (1 mrad/mCi), respectively. The brain to brain-absorbed dose was 0.0043 mGy/MBq (16 mrad/mCi).

Hickey et al. (41) in a 2005 study compared the measurement of myocardial perfusion using $[^{13}\text{N}]\text{NH}_3$ with that of $[^{15}\text{O}]\text{H}_2\text{O}$ in healthy volunteers, and they found that there was a discrepancy between the two measurements in a 2-compartment model analysis. The underestimation by $[^{13}\text{N}]\text{NH}_3$ was most likely attributable to the regional myocardial uptake variation and metabolism of $[^{13}\text{N}]\text{NH}_3$. This could be minimized by use of a 3-compartment model for data analysis. Other studies [PubMed] have shown the clinical utility of $[^{13}\text{N}]\text{NH}_3$ for quantification of myocardial blood flow in humans. In a study of 27 patients, Khorsand et al. (42) reported that gated cardiac $[^{13}\text{N}]\text{NH}_3$ imaging could be used for the estimation of LV function.

References

1. Clark JC, Aigbirdhio FI. Chemistry of nitrogen-13 and oxygen-15, in Handbook of Radiopharmaceuticals, M.J. Welch, C.S. Redvanly, Editor. 2003, John Wiley & Sons Inc.: Chichester, West Sussex, England. p. 119-140.
2. Phelps ME, Hoffman EJ, Raybaud C. Factors which affect cerebral uptake and retention of $^{13}\text{NH}_3$. Stroke 8(6):694–702; 1977. (PubMed)
3. Schelbert HR. PET studies of the heart., in Positron Emission Tomography and Autoradiography, M.E. Phelps, J.C. Mazziota and H.R. Schelbert, Editor. 1986, Raven Press: New York. p. 581-662.
4. Monahan WG, Tilbury RS, Laughlin JS. Uptake of ^{13}N -labeled ammonia. J Nucl Med 13(4):274–277; 1972. (PubMed)
5. Mudge GH. Agents affecting volume and composition of body fluids, in Goodman and Gilman's the pharmacological basis of therapeutics, A.G. Gilman, L.S. Goodman and A. Gilman, Editor. 1980, MacMillan Publishing Co., Inc.: New York. p. 869-870.
6. Walsh WF, Fill HR, Harper PV. Nitrogen-13-labeled ammonia for myocardial imaging. Semin Nucl Med 7 (1):59–66; 1977. (PubMed)
7. Straatmann MG. A look at ^{13}N and ^{15}O in radiopharmaceuticals. Int J Appl Radiat Isot 28(1-2):13–20; 1977. (PubMed)
8. Krivokapich J, Huang SC, Phelps ME, MacDonald NS, Shine KI. Dependence of $^{13}\text{NH}_3$ myocardial extraction and clearance on flow and metabolism. Am J Physiol 242(4):H536–H542; 1982. (PubMed)
9. Schelstraete K, Simons M, Deman J, Vermeulen FL, Slegers G, Vandecasteele C, Goethals P, De Schryver A. Uptake of ^{13}N -ammonia by human tumours as studied by positron emission tomography. Br J Radiol 55(659):797–804; 1982. (PubMed)
10. Joliot F, Curie I. Artificial production of a new kind of radio-element. Nature 133:201–202; 1934.
11. Lockwood AH, McDonald JM, Reiman RE, Gelbard AS, Laughlin JS, Duffy TE, Plum F. The dynamics of ammonia metabolism in man. Effects of liver disease and hyperammonemia. J Clin Invest 63(3):449–460; 1979. (PubMed)
12. Harper PV, Lathrop KA, Krizek H, Lembares N, Stark V, Hoffer PB. Clinical feasibility of myocardial imaging with $^{13}\text{NH}_3$. J Nucl Med 13(4):278–280; 1972. (PubMed)
13. van den Heuvel AF, Blanksma PK, Siebelink HM, van Wijk LM, Boomsma F, Vaalburg W, Crijns HJ, van Veldhuisen DJ. Impairment of myocardial blood flow reserve in patients with asymptomatic left ventricular dysfunction: effects of ACE-inhibition with perindopril. Int J Cardiovasc Imaging 17(5):353–359; 2001. (PubMed)

14. Ido T, Iwata R. Fully automated synthesis of $^{13}\text{NH}_3$. *J Labelled Comp Radiopharm* XVIII(1-2):244–246; 1981.
15. Wieland B, Bida G, Padgett H, Hendry G, Zippi E, Kabalka G, Morelle JL, Verbruggen R, Ghyoot M. In-target production of $[^{13}\text{N}]\text{ammonia}$ via proton irradiation of dilute aqueous ethanol and acetic acid mixtures. *Int J Rad Appl Instrum [A]* 42(11):1095–1098; 1991. (PubMed)
16. Berridge MS, Landmeier BJ. In-target production of $[^{13}\text{N}]\text{ammonia}$: target design, products, and operating parameters. *Appl Radiat Isot* 44(12):1433–1441; 1993. (PubMed)
17. Ferrieri RA, Schlyer DJ, Wieland BW, Wolf AP. On-line production of ^{13}N -nitrogen gas from a solid enriched ^{13}C -target and its application to ^{13}N -ammonia synthesis using microwave radiation. *Int J Appl Radiat Isot* 34(6):897–900; 1983.
18. Bida G, Wieland BW, Ruth TJ, Schmidt DG, Hendry GO, Keen RE. An economical target for nitrogen-13 production by proton bombardment of a slurry of C-^{13} powder in O-^{16} water. *J Labelled Compd Radiopharm* 23:1217–1218; 1986.
19. Welch MJ, Lifton JF. The fate of nitrogen-13 formed by the $^{12}\text{C}(\text{d},\text{n})^{13}\text{N}$ reaction in inorganic carbides. *J Am Chem Soc* 93(14):3385–3388; 1971.
20. Shefer RE, Hughey BJ, Klinkowstein RE, Welch MJ, Dence CS. A windowless ^{13}N production target for use with low energy deuteron accelerators. *Nucl Med Biol* 21(7):977–986; 1994. (PubMed)
21. Dence CS, Welch MJ, Hughey BJ, Shefer RE, Klinkowstein RE. Production of $[^{13}\text{N}]\text{ammonia}$ applicable to low energy accelerators. *Nucl Med Biol* 21(7):987–996; 1994. (PubMed)
22. Mulholland GK, Kilbourn MR, Moskwa JJ. Direct simultaneous production of $[^{15}\text{O}]\text{water}$ and $[^{13}\text{N}]\text{ammonia}$ or $[^{18}\text{F}]\text{fluoride ion}$ by 26 MeV proton irradiation of a double chamber water target. *Int J Rad Appl Instrum [A]* 41(12):1193–1199; 1990. (PubMed)
23. Suzuki K, Yoshida Y, Shikano N, Kubodera A. Development of an automated system for the quick production of ^{13}N -labeled compounds with high specific activity using anhydrous $[^{13}\text{N}]\text{NH}_3$ *Applied Radiation and Isotopes*, 50: p 1033-1038 1999.
24. Krasikova RN, Fedorova OS, Korsakov MV, Bennington BI, Berridge MS. Improved $[\text{N-}^{13}]\text{ammonia}$ yield from the proton irradiation of water using methane gas. *Appl Radiat Isot* 51:395–401; 1999.
25. Firouzbakht ML, Schlyer DJ, Wolf AP, Fowler JS. Mechanism of nitrogen-13-labeled ammonia formation in a cryogenic water target. *Nucl Med Biol* 26(4):437–441; 1999. (PubMed)
26. Krivokapich J, Barrio JR, Phelps ME, Watanabe CR, Keen RE, Padgett HC, Douglas A, Shine KI. Kinetic characterization of $^{13}\text{NH}_3$ and $[^{13}\text{N}]\text{glutamine}$ metabolism in rabbit heart. *Am J Physiol* 246(2 Pt 2):H267–H273; 1984. (PubMed)
27. Rauch B, Helus F, Grunze M, Braunwell E, Mall G, Hasselbach W, Kubler W. Kinetics of ^{13}N -ammonia uptake in myocardial single cells indicating potential limitations in its applicability as a marker of myocardial blood flow. *Circulation* 71(2):387–393; 1985. (PubMed)
28. Freed BR, McQuinn RL, Tilbury RS, Digenis GA. Distribution of ^{13}N in rat tissues following intravenous administration of nitroso-labeled BCNU. *Cancer Chemother Pharmacol* 10(1):16–21; 1982. (PubMed)
29. Cooper AJ, McDonald JM, Gelbard AS, Gledhill RF, Duffy TE. The metabolic fate of ^{13}N -labeled ammonia in rat brain. *J Biol Chem* 254(12):4982–4992; 1979. (PubMed)
30. Cooper AJ, Lai JC. Cerebral ammonia metabolism in normal and hyperammonemic rats. *Neurochem Pathol* 6(1-2):67–95; 1987. (PubMed)
31. Lockwood AH, Finn RD, Campbell JA, Richman TB. Factors that affect the uptake of ammonia by the brain: the blood-brain pH gradient. *Brain Res* 181(2):259–266; 1980. (PubMed)
32. Carter CC, Lifton JF, Welch MJ. Organ uptake and blood pH and concentration effects of ammonia in dogs determined with ammonia labeled with 10 minute half-lived nitrogen 13. *Neurology* 23(2):204–213; 1973. (PubMed)
33. Rosenspire KC, Schwaiger M, Mangner TJ, Hutchins GD, Sutorik A, Kuhl DE. Metabolic fate of $[^{13}\text{N}]\text{ammonia}$ in human and canine blood. *J Nucl Med* 31(2):163–167; 1990. (PubMed)

34. Schelbert HR, Phelps ME, Hoffman EJ, Huang SC, Selin CE, Kuhl DE. Regional myocardial perfusion assessed with N-13 labeled ammonia and positron emission computerized axial tomography. *Am J Cardiol* 43(2):209–218; 1979. (PubMed)
35. Schelbert HR, Phelps ME, Huang SC, MacDonald NS, Hansen H, Selin C, Kuhl DE. N-13 ammonia as an indicator of myocardial blood flow. *Circulation* 63(6):1259–1272; 1981. (PubMed)
36. Muzik O, Duvernoy C, Beanlands RS, Sawada S, Dayanikli F, Wolfe ER, Schwaiger M. Assessment of diagnostic performance of quantitative flow measurements in normal subjects and patients with angiographically documented coronary artery disease by means of nitrogen-13 ammonia and positron emission tomography. *J Am Coll Cardiol* 31(3):534–540; 1998. (PubMed)
37. Bol A, Melin JA, Vanoverschelde JL, Baudhuin T, Vogelaers D, De Pauw M, Michel C, Luxen A, Labar D, Cogneau M, et al. Direct comparison of $[^{13}\text{N}]\text{ammonia}$ and $[^{15}\text{O}]\text{water}$ estimates of perfusion with quantification of regional myocardial blood flow by microspheres. *Circulation* 87(2):512–525; 1993. (PubMed)
38. Weiss M, Roelsgaard K, Bender D, Keiding S. Determinants of $[^{13}\text{N}]\text{ammonia}$ kinetics in hepatic PET experiments: a minimal recirculatory model. *Eur J Nucl Med Mol Imaging* 29(12):1648–1656; 2002. (PubMed)
39. Raichle ME, Larson KB. The significance of the $\text{NH}_3\text{-NH}_4^+$ equilibrium on the passage of ^{13}N -ammonia from blood to brain. A new regional residue detection model. *Circ Res* 48(6 Pt 1):913–937; 1981. (PubMed)
40. Lockwood AH. Absorbed doses of radiation after an intravenous injection of N-13 ammonia in man: concise communication. *J Nucl Med* 21(3):276–278; 1980. (PubMed)
41. Hickey KT, Sciacca RR, Chou RL, Rodriguez O, Bokhari S, Bergmann SR. An improved model for the measurement of myocardial perfusion in human beings using N-13 ammonia. *J Nucl Cardiol* 12(3):311–317; 2005. (PubMed)
42. Khorsand A, Graf S, Eidherr H, Wadsak W, Kletter K, Sochor H, Schuster E, Porenta G. Gated Cardiac ^{13}N - NH_3 PET for Assessment of Left Ventricular Volumes, Mass, and Ejection Fraction: Comparison with Electrocardiography-Gated ^{18}F -FDG PET. *J Nucl Med* 46(12):2009–2013; 2005. (PubMed)